

Unexpected discovery of dichloroacetate derived adenosine triphosphate competitors targeting pyruvate dehydrogenase kinase to inhibit cancer proliferation

Shao-Lin Zhang, Xiaohui Hu, Wen Zhang, and Kin Yip Tam

J. Med. Chem., **Just Accepted Manuscript** • DOI: 10.1021/acs.jmedchem.5b01828 • Publication Date (Web): 23 Mar 2016

Downloaded from <http://pubs.acs.org> on March 25, 2016

Just Accepted

“Just Accepted” manuscripts have been peer-reviewed and accepted for publication. They are posted online prior to technical editing, formatting for publication and author proofing. The American Chemical Society provides “Just Accepted” as a free service to the research community to expedite the dissemination of scientific material as soon as possible after acceptance. “Just Accepted” manuscripts appear in full in PDF format accompanied by an HTML abstract. “Just Accepted” manuscripts have been fully peer reviewed, but should not be considered the official version of record. They are accessible to all readers and citable by the Digital Object Identifier (DOI®). “Just Accepted” is an optional service offered to authors. Therefore, the “Just Accepted” Web site may not include all articles that will be published in the journal. After a manuscript is technically edited and formatted, it will be removed from the “Just Accepted” Web site and published as an ASAP article. Note that technical editing may introduce minor changes to the manuscript text and/or graphics which could affect content, and all legal disclaimers and ethical guidelines that apply to the journal pertain. ACS cannot be held responsible for errors or consequences arising from the use of information contained in these “Just Accepted” manuscripts.

Unexpected discovery of dichloroacetate derived adenosine triphosphate competitors targeting pyruvate dehydrogenase kinase to inhibit cancer proliferation

Shao-Lin Zhang,[#] Xiaohui Hu,[#] Wen Zhang and Kin Yip Tam^{*}

Drug Development Core, Faculty of Health Sciences, University of Macau, Macau, China

ABSTRACT: Pyruvate dehydrogenase kinases (PDKs) have recently emerged as an attractive target for cancer therapy. Herein, we prepared a series of compounds derived from dichloroacetate (DCA) which inhibited cancer cells proliferation. For the first time, we have successfully developed DCA derived inhibitors that preferentially bind to the adenosine triphosphate (ATP) pocket of PDK isoform 1 (PDK1).

INTRODUCTION

Most cancer cells feature a switch in metabolism from mitochondrial oxidative phosphorylation to cytoplasmic aerobic glycolysis even under normoxia conditions.¹ Such metabolic remodeling is characterized by increased glycolysis and suppressed glucose oxidation, which provides cancer cells with proliferative advantages.²⁻⁴ Disruption of this unique metabolic pathway of cancer cells represents therapeutic opportunities in anticancer treatment.^{5,6}

PDKs function as a molecular switch that down-regulates mitochondrial respiration and enhance aerobic glycolysis *via* phosphorylating pyruvate dehydrogenase complex (PDC), a gate-keeper mitochondria enzyme, converting pyruvate to acetyl coenzyme A (acetyl-CoA).^{7,8} Inhibition of PDKs to increase the oxidative phosphorylation by activating PDC is an attractive therapeutic strategy to reverse the Warburg effect and inhibit cancer cell proliferation.⁹ Recently, four PDK isoforms (PDK1, PDK2, PDK3 and PDK4) in mitochondria have been isolated and characterized in terms of their differences in activity, tissue distribution and regulations.¹⁰ Among these isoforms, PDK1 is mostly associated with cancer malignancy. It had been reported that PDK1 was remarkably over-expressed in multiple human tumor such as lung cancer,¹¹ head squamous cancer,¹² myeloma¹³ and gastric cancer.¹⁴ PDK1 is transcriptionally regulated by oncogenes *c-MYC* and hypoxia-inducible factor 1 α (HIF-1 α) to control metabolic and malignant phenotypes of cancer cell.¹⁵ Collectively, it has been suggested that PDK1 is a viable anticancer target.¹⁶

So far, four types of inhibitors have been reported to inhibit the activity of PDKs *via* different mechanisms. As show in Figure 1, Nov3r¹⁷ and **1** (AZD7545)¹⁸ are the PDK2 inhibitors with the same warhead, namely the trifluoromethylpropanamide group, which binds to the lipoamide-binding site located at one end of the R domain of PDKs. In contrast, Pfz3¹⁹ binds to PDKs at the other end of R domain of the N terminus opposing the lipoamide-binding site. VER-246608²⁰ and Radicicol²¹ are ATP-competitive inhibitors, which down regu-

late the kinase activity by binding to the ATP pocket. DCA, a structural analogue of PDC substrate pyruvate, binds to the pyruvate-binding site in the center of the R domain to regulate the activity of PDKs.²² In 2007, Michelakis *et al*²³ first reported that DCA could inhibit the growth of cancer cells. Since then, DCA has become a hot molecule and received an increasing attention. However, its low binding affinity to PDKs requires a high dose to become efficacious, which appeared to limit its clinic application. Moreover, the clinical records suggested that patients receiving long-term DCA treatment showed reversible limb motor weakness and demyelination of cerebral and cerebellar white matter.²⁴ It is highly desirable to modify DCA to offer more potent anticancer agents. Recently, series of DCA derivatives have been developed, however, none of their action mechanisms had been explained explicitly.^{9, 25-27}

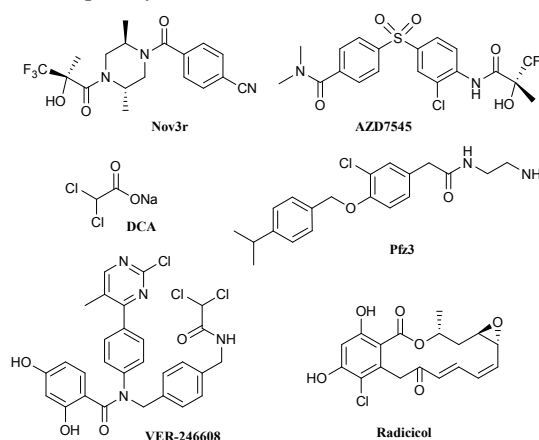
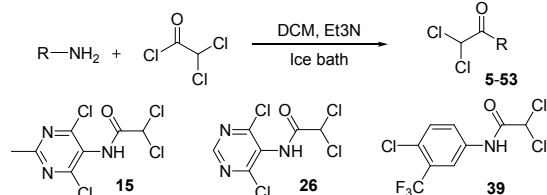


Figure 1 Structures of known PDKs inhibitors

In this paper, we prepared series of DCA analogues with the aim to find new inhibitors with better inhibitory potency and stronger binding interactions than that of DCA. We found that the DCA based inhibitors bind to the ATP pocket, but not presumed pyruvate pocket.

RESULTS AND DISCUSSION

Modification of DCA leads to potent compounds that inhibit cancer cells proliferation. According to the literature,^{25,26} the carboxyl group is the only modifiable site in DCA without detrimental effect on its anti-cancer property. With this notion in mind, we designed a chemical series by modifying the carboxyl group to study the anti-proliferation potency against cancer cells. We synthesized and purified about 50 novel DCA analogues (see Scheme 1), whose structures were confirmed by ¹H NMR, ¹³C NMR and HRMS spectra (see SI).



Scheme 1 General synthetic route for target compounds 5–53. R groups represent as substituted aromatic rings, such as benzene, pyrimidine and pyridine rings, etc (detailed information was listed in SI).

We then tested their anti-proliferative activity against the *human lung adenocarcinoma* epithelial cell line (A549) and

breast cancer cell line Michigan Cancer Foundation-7 (MCF-7) by using MTT assay. We identified three hit compounds **15**, **26** and **39**, which completely inhibited the growth of the cancer cells at 40 μ M. The inhibition was also confirmed by black field pictures of the cultured cells acquired from IncuCyte Zoom (Essen Biosciences) (see Figure S1). Compared with DCA, **15** and **26** exhibited a very low IC₅₀ values, about 1000-fold more potent against A549 and MCF-7. Excitingly, **39** was found to be 3000-fold more potent than DCA against these two cell lines (see Table 1, Figure S2). We further evaluated the inhibition rate of the compounds to normal human breast cell MCF-10a, where the compounds showed relative low cytotoxic effects. The inhibition rate was only 10.32% for **39** at the concentration of 20 μ M (see Table 1). In order to study the mode of cell death, **15**, **26** and **39** were used to induce MCF-7 apoptosis and examined by Annexin V-FITC/PI FACS assay. As shown in the Figure 2, the percentages of apoptosis for MCF-7 cells treated with **15**, **26** and **39** at 20 μ M for 10 h were 9.87%, 10.60% and 11.80%, respectively, which outperformed DCA at 10 mM. When time increased to 15 h, the apoptosis rate was 14.2% for **39**, suggesting the induction of apoptosis in MCF-7 by **39** follows a time-dependent manner.

Table 1 *In vitro* activity of the selected compounds on A549 and MCF-7, and human normal cell line MCF-10a.

Compounds	IC ₅₀ (μ M) ^a		Inhibition rate (%) for MCF-10a		K _d (μ M) ^b
	A549	MCF-7	10 μ M	40 μ M	
15	26.02 \pm 1.15	22.89 \pm 1.44	7.57	41.56	NT ^c
26	28.42 \pm 0.98	19.34 \pm 1.06	4.91	42.36	NT ^c
39	7.46 \pm 0.81	3.12 \pm 0.20	3.51	10.32 (20 μ M)	40.8
DCA	23.58 \pm 1.26 (mM)	12.35 \pm 0.74 (mM)	3.42 (20 μ M)	41.10 (10 mM)	> 1000

^a IC₅₀ is the 50% inhibitory concentration. ^b Dissociation constants (K_d) shows the binding affinity of the inhibitor to the PDK1, which were determined by ITC described in experimental procedures (Figure S1). ^c Not test.

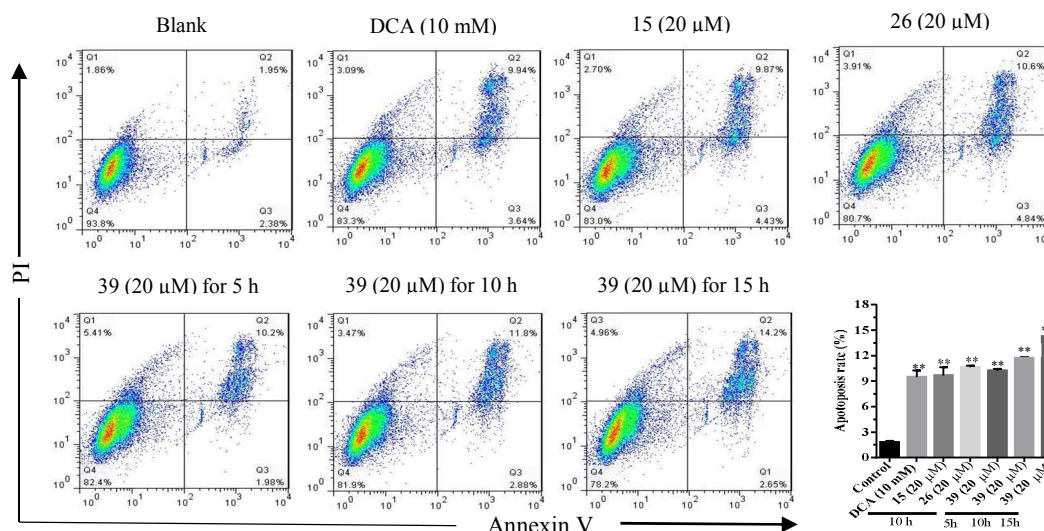


Figure 2 Flow cytometer analysis using FITC Annexin V apoptosis detection Kit with PI. The cells were treated with DCA, **15**, **26** and **39** for different time, and then stained with the kit. Cells in the lower right quadrant indicate Annexin V-positive/PI negative, early apoptotic cells. The cells in the upper right quadrant indicate Annexin V-positive/PI positive, late apoptotic or necrotic cells. * $P < 0.05$, versus control group.

Compound 39 binds to PDK1. With the improved anticancer activity of **39** and others, we would like to address the question whether the compound interacts with its supposed target PDKs. PDK1 solution was titrated with **39** in an isothermal calorimetry experiment, a moderate K_d (40.8 μ M) was derived, indicating that **39** interacts directly with PDK1 (see Figure 3A). PDK1 has four known binding pockets.⁷ To date, no

unambiguous evidence refers to the binding mode for DCA analogues other than a plausible pyruvate binding pocket that based on the crystal structure of DCA and PDK protein.²² To rationalize the binding process, **39** was docked into the pyruvate pocket of PDK1 by Sybyl-X-2.1. A negative total binding scores (-7.81) and physical hindrance of the pocket in the model led us to believe that it is unlikely for **39** to bind to this

pocket. To explore which binding pocket(s) that **39** is likely to bind, we then performed a series of competitive titration experiments. Specifically, we titrated PDK1 with adenosine diphosphate (ADP) (in the absence of **39**, Figure 3B). The K_d value was $4.27 \mu\text{M}$ ($K_a = 234000$) with a Gibbs free energy (ΔG) of -7325.6 J/mol . However, in the presence of **39**, the K_d value increased to $7.87 \mu\text{M}$ ($K_a = 127000$, Figure 3C), and more importantly, ΔG value dropped to -6965.2 J/mol , indicating pre-occupation of the ATP pocket by **39**. Titration of PDK1 with **1** in the presence or absence of **39** did not show any discrepancy in K_d or ΔG values (Figure 3D and 3E). Hence it is unlikely that **39** is competing with **1** for the lipoamide-binding site. Acetyl-CoA binding to PDK1 was undetectable under the same experimental conditions. All together, these observations suggest that **39** binds to an unexpected ATP pocket in PDK1. To the best of our knowledge, this is the first report of DCA analogues binding to an ATP pocket in PDK1.

Compounds 15, 26 and 39 activate PDC. Inhibition of PDK1 leads to PDC activation. Firstly, PDK1 kinase activity was evaluated in the presence of DCA, **15**, **26** and **39** using a commercial kit (see SI). As shown in Figure S3, **15**, **26** and **39** at $50 \mu\text{M}$ reduced the consumption of ATP, which was used to phosphorylate peptide fragment around Ser293 site of PDC by PDK1, suggesting **15**, **26**, and **39** inhibit PDK1 activity. Next

we turn our attention to study **15**, **26** and **39** on PDC activation. Kinetic experiments were carried out by measuring the formation of reduced nicotinamide adenine dinucleotide (NADH) during the course of pyruvate conversion to acetyl-CoA. To our surprise, **15**, **26** and **39** at $50 \mu\text{M}$ barely activated PDC when ATP was included in the reaction mixture, while 10 mM DCA could slightly activate PDC (see Figure 4A). Interestingly, in the absence of ATP, the activity of PDC was enhanced by the addition **15**, **26** and **39**, suggesting these compounds could serve as PDC activators (see Figure 4B). However, it was still not clear whether they activate PDC directly or *via* the inhibition of PDKs. To address this question, we examined PDC activity by adding recombinant PDK1, which was able to inhibit PDC activity completely (see Figure 4C). When **15**, **26** and **39** were added to the mixture, the activity of PDC was restored to a large extent. This observation provides a strong evidence to suggest that **15**, **26** and **39** act through PDK1 to activate PDC. Inability of **15**, **26** and **39** to activate PDC in the presence of ATP could be explained by their relative low binding affinity to PDK1 as compared with ATP. Moreover, we found that the phosphorylation of PDC by PDK1 was inhibited by compounds **15**, **26** and **39**, as well as DCA (see Fig S4), another proof of their regulation PDC *via* kinase inhibition.

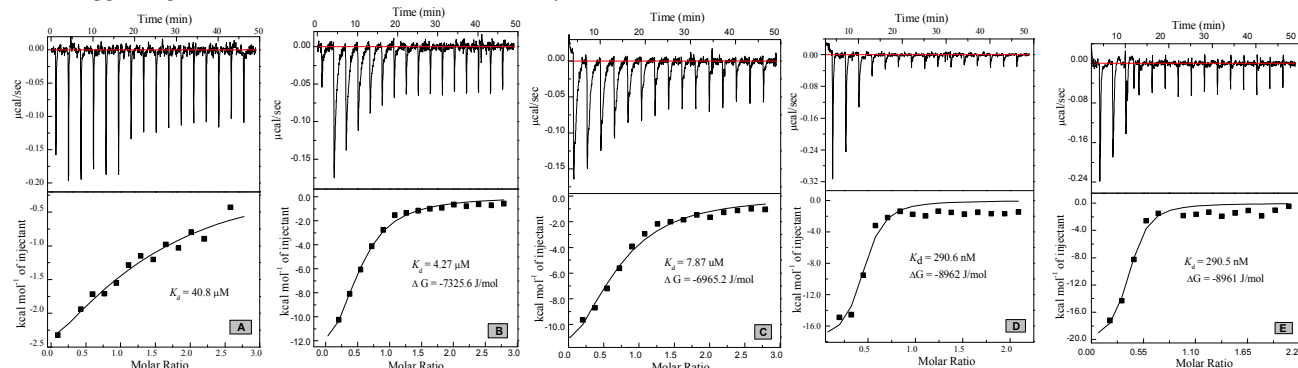


Figure 3 ITC analysis of the binding mode for **39** and PDK1, raw data for the titration, in which the power output in microcalories per second is measured as function of time in minutes. A: **39** ($100 \mu\text{M}$) was titrated into the PDK1 ($20 \mu\text{M}$) solution; B: ADP ($55 \mu\text{M}$) was titrated into the PDK1 ($20 \mu\text{M}$) solution; C: PDK1 ($20 \mu\text{M}$) solution and **39** ($50 \mu\text{M}$) solution and ADP ($55 \mu\text{M}$) was added into the mixture; D: **1** ($40 \mu\text{M}$) was titrated into the PDK1 ($10 \mu\text{M}$) solution; E: PDK1 ($10 \mu\text{M}$) and **39** ($50 \mu\text{M}$) mix together, then **1** was titrated into the mixture.

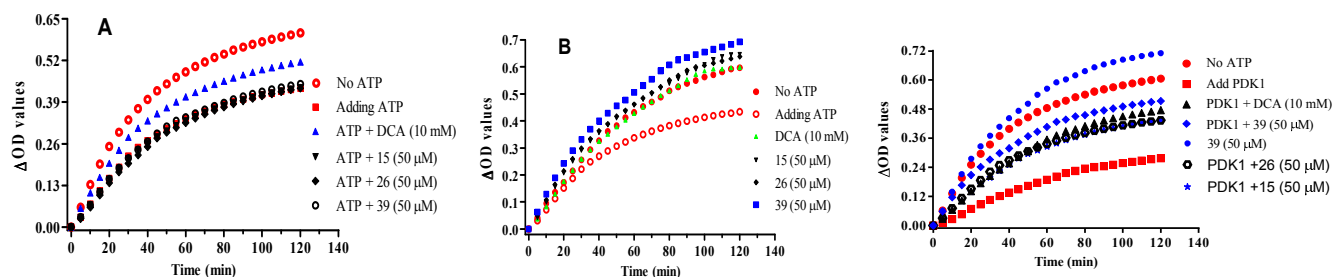


Figure 4 Compounds **15**, **26** and **39** effect on PDC kinetics, $OD_{340 \text{ nm}}$ values were read at $37 \text{ }^\circ\text{C}$. A: **15**, **26** and **39** with ATP incubated with PDC at 96-well plate; B: **15**, **26** and **39** without ATP were incubated in the 96-well plate; C: PDK1, DCA, **15**, **26**, **39** and their mixture were added into the PDC solution.

Compounds 15, 26 and 39 alter the mitochondrial bioenergetics in MCF-7. Inhibition of PDK1 activates PDC, leading to a switch of pyruvate consumption from lactate production to oxidative phosphorylation to form acetyl-CoA in the mitochondrion. The oxygen consumption and the degree of acidification will change in cancer cells because of abnormal pyruvate metabolism. The metabolic modulatory effect of **15**, **26** and **39** were evaluated by measuring the oxygen consumption

rate (OCR) and extracellular acidification (ECAR) on a Seahorse XFe24 extracellular flux analyzer, and the lactate production was measured by Nova Bioprofile Flex analyzer (Nova Biomedical). As shown in Figure 5, OCR was increased when the cells were treated with $20 \mu\text{M}$ of **15**, **26** and **39**. Especially for **39**, the enhancement in OCR is much more significant than that of DCA at 10 mM . ECAR was significantly decreased with the addition of **15**, **26** and **39**, which can be

explained by the reduction of glycolysis in the cancer cells. As expected, the proton production rate (PPR) was decreased in a similar fashion as ECAR. We further compared the ratio of OCR/ECAR. OCR/ECAR was dramatically increased by **15**, **26** and **39**. As shown in the Figure 5E, 5F and 5G, except for

the highest dose for **39**, we observed a dose-dependent increase in OCR and decrease in ECAR and PPR in MCF-7 of response to **39**. In Figure 5H, lactate production was decreased by **39** at 20 μM after 12 h treatment, which is consistent with the ECAR change.

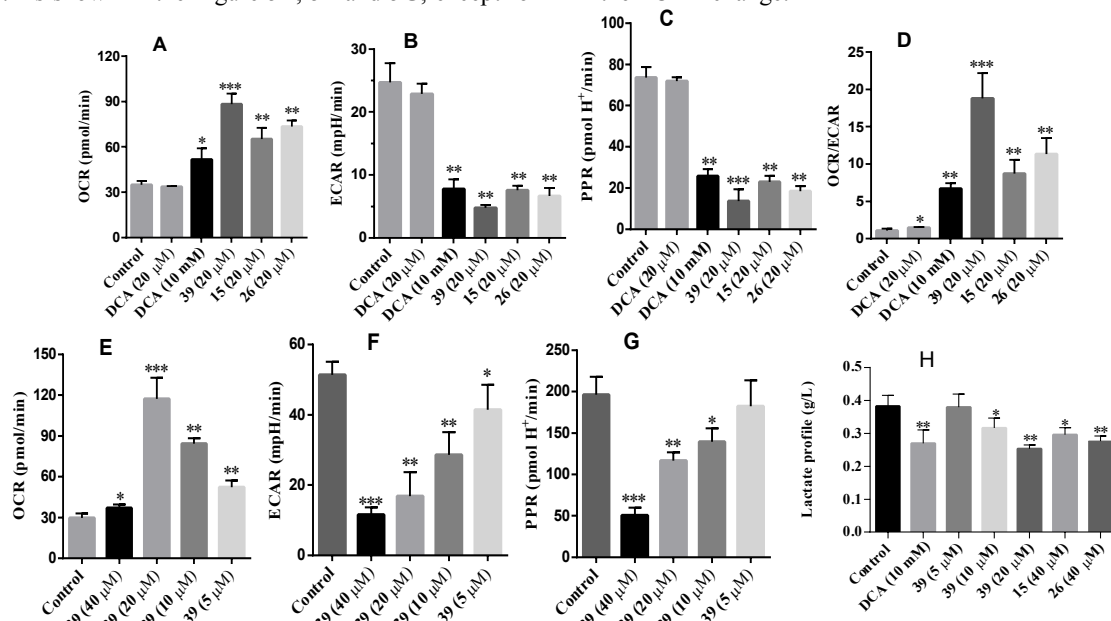


Figure 5 Effect of DCA, **15**, **26** and **39** on MCF-7 cell glycolysis. MCF-7 cells (27000/well) were treated with 20 μM and 10 mM DCA, 20 μM **15**, **26** and **39** for 12 h. A: OCR was increased with the treatment of DCA, **15**, **26** and **39**; B: ECAR was significantly decreased by DCA, **15**, **26** and **39**; C: PPR was decreased with adding DCA, **15**, **26** and **39**; as ECAR; D: Ratio of OCR/ECAR was significantly increased by treatment of **15**, **26** and **39**; E: OCR was dose-dependent increased with the concentration of **39** increases except at the highest dose of **39**; F: ECAR was dose-dependent decreased with concentration of **39** increases; G: PPR was decreased with the concentration of **39** increases. H: Lactate formation was decreased by treatment of **15**, **26** and **39**. * $P < 0.05$, versus untreated control group.

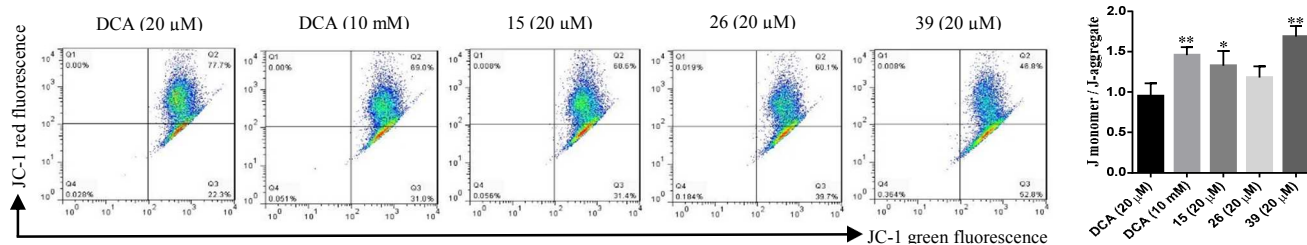


Figure 6 Change in the $\Delta\psi\text{m}$ by JC-1 assay. Treatment of MCF-7 with DCA, **15**, **26** and **39** led to the decrease of $\Delta\psi\text{m}$ in the cancer cells. Cells were stained with JC-1, the green fluorescence represents depolarized mitochondria (J-monomer), and the red fluorescence represents the hyperpolarized mitochondria (J-aggregates). The depolarization of $\Delta\psi\text{m}$ is indicated by the increase in the ratio of J monomer / J aggregate. * $P < 0.05$, versus the group with the treatment of DCA at 20 μM .

Compounds 15, 26 and 39 reverse mitochondria hyperpolarization in cancer cell. Cancer cells exhibit hyperpolarized mitochondrial membrane potential ($\Delta\psi\text{m}$) compared with normal cells, in which a positive voltage gradient exists across the inner mitochondrial membrane from the outside.²⁷ Depolarization of cancer cell represents an effective strategy to inhibit cancer cell growth by introducing apoptosis.²³ Here we investigated the effect of **15**, **26** and **39** on $\Delta\psi\text{m}$ of cancer cells using a cationic dye, 5,5',6,6'-tetrachloro-1,1',3,3'-tetraethylbenzimidazolylcarbocyanine iodide (JC-1), which accumulated in mitochondria accompanied by a fluorescence emission shift from green to red due to the formation of red fluorescent J-aggregates. Mitochondria depolarization is indicated by increase in the ratio of green / red fluorescence intensity. In this experiment, MCF-7 cells were treated with DCA (20 μM and 10 mM), **15** (20 μM), **26** (20 μM) and **39** (20 μM)

for 12 h, followed by staining with JC-1. As shown in the Figure 6, the quantitative analysis of JC-1 stained MCF-7 by **15**, **26** and **39** revealed a significant decrease in the red (high $\Delta\psi\text{m}$) to green (low $\Delta\psi\text{m}$) ratio compared with the cells that treatment of DCA at an equivalent concentration at 20 mM. This was also observed in the JC-1 imaging experiment (see Figure S5). Compound **39** showed a J-monomer / J-aggregate ratio at 1.69 (Figure 6), which was significantly higher than the ratio given by DCA at 10 mM. Meanwhile, **39** treated cells displayed a reduction of $\Delta\psi\text{m}$ in dose-dependent manner (see Figure 7). All this suggested that **15**, **26** and **39** reverse mitochondria hyperpolarization and oxidative metabolism suppression in cancer cell. To further validate this result, MCF-7 cells were stained by tetramethyl rhodamine methyl ester (TMRM), a fluorescent dye, which accumulate in the hyperpolarized cells. The **15**, **26** and **39** treated MCF-7 cells showed a reduc-

tion of red fluorescent signal (see Figure S6), suggesting **15**, **26** and **39** led to mitochondrial potential depolarization in MCF-7 cells. Our results suggest that **15**, **26** and **39** provide apoptotic stimuli for MCF-7 cells through mitochondrial membrane depolarization, which could lead to the cancer cells apoptosis.

CONCLUSION

In this paper, a series of DCA analogues were synthesized and their structures were confirmed by ^1H NMR, ^{13}C NMR and HRMS. Biological assay revealed that three potent compounds, namely **15**, **26** and **39** inhibited the cancer cells proliferation at

micromolar concentrations. Kinetic studies demonstrated that **15**, **26** and **39** serve as a PDC activators through inhibition of PDK1. ITC experiments suggested that **39** binds to ATP binding pocket instead of the pyruvate binding pocket in PDK1. The mitochondria bioenergetics measurement revealed that **15**, **26** and **39** could serve as a potential modulator to reprogram the glucose metabolism of cancer cells from lactate formation to oxidative phosphorylation. Additionally, **15**, **26** and **39** were found to depolarize the mitochondria membrane potential of cancer cell, which could evolve into apoptotic stimuli leading to cell death.

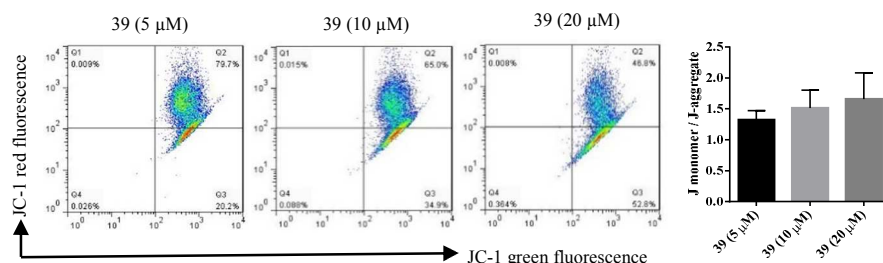


Figure 7 Depolarization of $\Delta\psi_m$ in MCF-7 cells by **39**. The cells were treated with **39** for 12 h before measurement.

EXPERIMENTAL SECTION

Materials and Methods. All the building blocks were bought from sigma, JK chemical, Wako and Acros and were used as received. Solvents were purchased from Anqua Chemicals Supply (ACS Grade). Dimethylsulfoxide- d_6 was bought from CIL, USA. All the new compounds were characterized by ^1H NMR, ^{13}C NMR and HRMS. NMR spectra were recorded on a Bruker AV-400 instrument and reported in ppm downfield from DMSO (2.50 ppm), and all ^{13}C NMR spectra are reported in ppm relative to residual DMSO (39.6 ppm). Coupling constants are reported in Hz with multiplicities denoted as s (singlet), d (doublet), t (triplet), q (quartet) and m (multiplet). Reactions were monitored by thin-layer chromatography (TLC) carried out on commercial silica gel plates (GF254) using UV light as a visualizing agent. High resolution mass spectra (HRMS) were obtained on a Xevo G2-XS QToF spectrometer. All of the tested compounds exhibited purities of > 95 % as determined by peak area integration in reverse phase chromatography through a C-18 column (Agilent HPLC 1260, USA).

Synthesis of the 2,2-dichloro-N-(4,6-dichloro-2-methylpyrimidin-5-yl)acetamide (15). A mixture of 4,6-dichloro-2-methylpyrimidin-5-amine (1.77 g, 10 mmol) and Et_3N (1.67 mL, 12 mmol) were stirred in the DCM (20 mL) at ice bath. Then 2, 2-dichloroacetyl chloride (1.06 mL, 11 mmol) was added with dropwise. After completion of the reaction, the mixture was extracted with saturated brine (3 x 30 mL), then the combined organic phase was dried over anhydrous sodium sulfate and subsequently the solvent was evaporated under reduced pressure. The residue was purified by silica gel column chromatography (eluent, petroleum/ethyl acetate, 10/1, V/V) to obtain **15** (2.20 g) as pale yellow solid. Yield: 78.5 %. Purity: 95.78 %. m.p. 148–149 °C. ^1H NMR (400 MHz, $\text{DMSO}-d_6$): δ 10.97 (s, 1H), 6.82 (s, 1H), 2.65 (s, 3H) ppm; ^{13}C NMR (100 MHz, $\text{DMSO}-d_6$): δ 167.14, 162.69, 159.31, 124.84, 66.71, 25.00; HRMS (ESI) calcd. for $\text{C}_7\text{H}_6\text{Cl}_4\text{N}_3\text{O}$ $[\text{M}+\text{H}]^+$, 287.9265; found, 287.9259.

2,2-dichloro-N-(4,6-dichloropyrimidin-5-yl)acetamide (26). Compound **26** was prepared according to the experimental

procedure for compound **15**, starting from 4,6-dichloropyrimidin-5-amine (1.63 g, 10 mmol), 2-dichloroacetyl chloride (1.06 mL, 11 mmol) and Et_3N (1.67 mL, 12 mmol). The desired compound (1.26 g) was obtained as light yellow solid. Yield: 47.1 %. Purity: 96.71 %. m.p. 107–108 °C. ^1H NMR (400 MHz, $\text{DMSO}-d_6$): δ 11.12 (s, 1H), 8.93 (s, 1H), 6.85 (s, 1H) ppm; ^{13}C NMR (100 MHz, $\text{DMSO}-d_6$): δ 162.59, 159.78, 156.83, 127.92, 66.13; HRMS (ESI) calcd. for $\text{C}_6\text{H}_4\text{Cl}_4\text{N}_3\text{O}$ $[\text{M}+\text{H}]^+$, 273.9108; found, 273.9115.

2,2-dichloro-N-(4-chloro-3-(trifluoromethyl)phenyl)acetamide (39). Compound **39** was prepared according to the experimental procedure for compound **15**, starting from 4-chloro-3-(trifluoromethyl)aniline (0.98 g, 5 mmol), 2-dichloroacetyl chloride (0.53 mL, 5.5 mmol) and Et_3N (0.84 mL, 6 mmol). The desired compound (0.85 g) was obtained as yellow solid. Yield: 56.0 %. Purity: 98.64 %. m.p. 96–97 °C. ^1H NMR (400 MHz, $\text{DMSO}-d_6$): δ 11.09 (s, 1H), 8.14 (d, 1H, $J = 2.4$ Hz), 7.88 (dd, 1H, $J = 2.8, 8.8$ Hz), 7.70 (d, 1H, $J = 8.8$ Hz), 6.62 (s, 1H) ppm; ^{13}C NMR (100 MHz, $\text{DMSO}-d_6$): δ 162.45, 137.22, 132.50, 127.54, 127.23, 126.93, 126.62, 125.64, 124.80, 123.99, 121.27, 118.75, 118.64, 118.58, 67.23. HRMS (ESI) calcd. for $\text{C}_9\text{H}_6\text{Cl}_2\text{F}_3\text{NO}$ $[\text{M}+\text{H}]^+$, 305.9467; found, 305.9460.

Apoptosis detection by flow cytometry. MCF-7 cells were seeded at a density of 2×10^5 cells/mL on each well of a six well plate and were allowed to grow overnight. Cells were treated with 10 mM DCA, 20 μM **15**, **26** and **39** for 12 h at 37 °C. Additional, time-dependent experiments for studying the apoptosis induced by **39** were pursued at 5 h, 10 h and 15 h. For each time point, cells were trypsinized, repeatedly washed with cold PBS for three times, and centrifuged at 800 RPM for 5 min, and the supernatants were discarded. Cells were resuspended in 1 x Annexin binding buffer to $\sim 5 \times 10^5$ cells/mL, preparing a sufficient volume to have 100 μL per assay. To 100 μL of cell suspension, 10 μL Annexin V and 5 μL PI working solution were added, and incubated for 15 min at room temperature. After incubation, 400 μL PBS was added to

each sample, and was gently mixed and analyzed immediately on the flow cytometer.

PDK1 expression and purification. Human PDK1 (aa29-436) was cloned from pDONR223-PDK1 (Addgene plasmid #23804) using primers (tacttccaatccaatgcatcgactcggtctc and ttatccacttccaatgttattactaggcactgcgga-ac) and ligated into pET-His6Sumo-TEV-LIC (Addgene plasmid #29659). N-terminal 6xHis-SUMO tagged recombinant was co-expressed with chaperonins GroEL and GroES (encoded by Addgene plasmid #27396) in *Escherichia coli* BL-21 cells, purified (> 95 %) through a nickel-charged HiTrap IMAC column and a HiLoad 16/600 Superdex200 column on an AKTA Avant150 chromatography system.

Kinetic study for the PDC. PDK inhibition activity was assessed indirectly by measuring the residual PDC activity after kinase reaction in an assay, in which the NADH was measured during the conversion from pyruvate to the acetyl-CoA. The assay consisted of the following three steps. (1) Preincubation. This step was included in the assay because the intrinsic PDK activity of commercially available PDC was enhanced by up to 2.7-fold. Pig PDC (sigma, CAS 9014-20-4) containing intrinsic kinase activity PDKs was incubated for 40 min at 37 °C in buffer A [40 mM Mops (pH 7.20), 0.5 mM EDTA, 30 mM KCl, 1.5 mM MgCl₂, 0.25 mM acetyl-CoA, 0.05 mM NADH, 2 mM dithiothreitol, 10 mM NaF] at a concentration of 80 µg/ml. (2) PDK reaction. The PDK reaction was performed in a total volume of 100 µL at 37 °C, and was initiated by diluting the PDC mixture 2.2-fold in 1.8 x buffer A containing 55 µM ADP, 100 µM ATP (ATP was omitted in control reactions representing complete PDK inactivation). After 3 min the kinase reaction was terminated by the addition of 10 µL of stopping buffer (55 mM ADP and 55 mM pyruvate). (3) Residual PDC activity. The remaining PDC activity was tested in a total volume of 200 µL at 37 °C by addition of 90 µL of buffer B [120 mM Tris (pH 7.8), 0.61 mM EDTA, 0.73 mM MgCl₂, 2.2 mM thiamine pyrophosphate, 11 mM 2-mercaptoethanol, 2.2 mM NAD⁺, 2.2 mM pyruvate, 1.1 mM CoA] by measuring the production of NADH at 340 nm.

ITC analysis. The concentration of PDK1 proteins were determined by NanoDrop 2000 and diluted to 10 µM solutions in the buffer solution containing 50 mM KH₂PO₄/K₂HPO₄, pH 7.4, 250 mM KCl, 2 mM MgCl₂. Stock solutions of the synthesized PDK1 inhibitor **39** and the commercially available compound **1** were prepared in DMSO (40–100 mM). ATP, ADP and acetyl-CoA were dissolved in double-distilled water to the concentrations of 10 mM, 55 mM and 5 mM, respectively. Then the above mentioned solutions were diluted by buffer solution (50 mM KH₂PO₄/K₂HPO₄, pH 7.4, 250 mM KCl, 2 mM MgCl₂) into the desired concentrations containing 1 % DMSO. The corresponding solutions were delivered into the titration syringe. ITC experiments were accomplished using a Microcal iTC₂₀₀ microcalorimeter (GE Healthcare). The reaction cell contained 300 µL PDK1. Titrations were performed with the injection of 2.5 µL titrant(s) for every increment into the reaction cell which maintained at 25 °C. All of the ITC data were initially analyzed and the baseline was automatically determined by the Origin 7, then followed by curve-fitting to one-site model to obtain binding parameters ΔG , ΔH , ΔS and n .

Seahorse XF24 mitochondria bioenergetics assay. The key parameter of glycolytic function was assessed using a Seahorse XF glycolysis stress kit. Prior to the assay, XF sensor cartridges were hydrated. To each well of an XF utility plate, 1 mL of Seahorse Bioscience calibrant was added and the XF

sensor cartridge was placed on top of the utility plate, and kept at 37 °C without CO₂ for 12 h. MCF-7 cells were cultured in XF24-well cell culture microplates (Seahorse Bioscience) at a density of 2.7 x 10⁴ cells/well in 100 µL growth medium and incubated for 1 h at 37 °C in 5% CO₂ atmosphere. After the cells were attached, an additional 100 µL growth medium was added and the cells were incubated for 24 h at 37 °C in 5% CO₂ atmosphere. The cells were treated with DCA (20 µM and 10 mM), **15** and **26** (20 µM), **39** (5 µM, 10 µM and 20 µM) for 12 h at 37 °C in 5% CO₂ atmosphere. After 12 h, the culture was removed from each well (retaining 50 µL) and the cells were rinsed two times with 1000 µL of XF stress test glycolysis optimization medium pre-warmed to 37 °C and finally 1000 µL of optimization medium was added to each well and the plate was placed at 37 °C without CO₂ for 1 h prior to assay. The OCR, a measure of mitochondrial respiration, and the ECAR and PPR, markers for glycolysis, were measured simultaneously for 16 min to establish a baseline rate.

ASSOCIATED CONTENT

Supporting Information: Cell culture, cell cytotoxic assay, IncuCyte Zoom live cell images, lactate measurement, PDK kinase activity assay, TMRM assay, JC-1 assay for image, Figures (Figs. S1-S6), Table S1 and ¹H NMR, ¹³C NMR, HRMS and HPLC spectra were listed in supporting information. This material is available free of charge via the Internet at <http://pubs.acs.org>.

AUTHOR INFORMATION

* Corresponding Author

Prof. Kin Yip Tam (kintam@umac.mo); Tel.: +853 88224988; fax: +853 88222314.

Author Contributions

These authors contributed equally to this study.

Notes

The authors declare no competing financial interests.

ACKNOWLEDGMENT

We thank the financial support from the Science and Technology Development Fund, Macao S.A.R (FDCT) (project reference no. 086/2014/A2).

ABBREVIATIONS USED

DCA, dichloroacetate; PDK, Pyruvate dehydrogenase kinase; PDC, pyruvate dehydrogenase complex; ATP, adenosine triphosphate; ADP, adenosine diphosphate; acetyl-CoA, acetyl coenzyme A; HIF-1 α , hypoxia-inducible factor 1 α ; OCR, oxygen consumption rate; ECAR, extracellular acidification; PPR, proton production rate; $\Delta\psi_m$, mitochondrial membrane potential; TMRM, tetramethyl rhodamine methyl ester; NADH, reduced nicotinamide adenine dinucleotide; A549, *human lung adenocarcinoma* epithelial cell line; MCF-7, breast cancer cell line Michigan Cancer Foundation-7.

REFERENCES

- (1) Vander Heiden, M. G.; Cantley, L. C.; Thompson, C. B. Understanding the Warburg effect: the metabolic requirements of cell proliferation. *Science*, **2009**, *22*, 1029–1033.
- (2) Michelakis, E. D.; Sutendra, G.; Dromparis, P.; Webster, L.; Haromy, A.; Niven, E.; Maguire, C.; Gammer, T.-L.; Mackey, J. R.; Fulton, D.; Abdulkarim, B.; McMurtry M. S.; Petruk, K. C. Metabolic

- modulation of glioblastoma with dichloroacetate. *Sci. Transl. Med.*, **2010**, *2*, 31ra34.
- (3) Samudio, I.; Fiegl, M.; Andreeff, M. Mitochondrial uncoupling and the Warburg effect: molecular basis for the reprogramming of cancer cell metabolism. *Cancer Res.*, **2009**, *69*, 2163–2166.
- (4) Dhar, S.; Lippard, S. J. Mitaplatin, a potent fusion of cisplatin and the orphan drug dichloroacetate. *Proc. Natl. Acad. Sci. U S A*, **2009**, *106*, 22199–22204.
- (5) Meng, T.; Zhang, D. D.; Xie, Z. Q.; Yu, T.; Wu, S. C.; Wyder, L.; Regenass, U.; Hilpert, K.; Huang, M.; Geng, M. Y.; Shen, J. K. Discovery and optimization of 4,5-diarylisoxazoles as potent dual inhibitors of pyruvate dehydrogenase kinase and heat shock protein 90. *J. Med. Chem.*, **2014**, *57*, 9832–9843.
- (6) (a) Vander Heiden, M. G. Targeting cancer metabolism: a therapeutic window opens. *Nat. Rev. Drug Discov.*, **2011**, *10*, 671–684; (b) Sun, W.; Xie, Z.; Liu, Y.; Zhao, D.; Wu, Z.; Zhang, D.; Lv, H.; Tang, S.; Jin, N.; Jiang, H.; Tan, M.; Ding, J.; Luo, C.; Li, J.; Huang, M.; Geng, M. JX06 selectively inhibits pyruvate dehydrogenase kinase PDK1 by a covalent cysteine modification. *Cancer Res.*, **2015**, doi: 10.1158/0008-5472.CAN-15-1023.
- (7) Zhang, S. L.; Hu, X.; Zhang, W.; Yao, H. K.; Tam, K. Y. Development of pyruvate dehydrogenase kinase inhibitors in medicinal chemistry with particular emphasis as anticancer agents. *Drug Discov. Today*, **2015**, *20*, 1112–1119.
- (8) Tso, S. C.; Qi, X.; Gui, W. J.; Wu, C. Y.; Chuang, J. L.; Wernstedt-Asterholm, I.; Morlock, L. K.; Owens, K. R.; Scherer, P. E.; Williams, N. S.; Tambar, U. K.; Wynn, R. M.; Chuang, D. T. Structure-guided development of specific pyruvate dehydrogenase kinase inhibitors targeting the ATP-binding pocket. *J. Biol. Chem.*, **2014**, *289*, 4432–4443.
- (9) (a) McFate, T.; Mohyeldin, A.; Lu, H.; Thakar, J.; Henriques, J.; Halim, N. D.; Wu, H.; Schell, M. J.; Tsang, T. M.; Teahan, O.; Zhou, S.; Califano, J. A.; Jeoung, N. H.; Harris, R. A.; Verma, A. Pyruvate dehydrogenase complex activity controls metabolic and malignant phenotype in cancer cells. *J. Biol. Chem.*, **2008**, *283*, 22700–22708; (b) Saha, S.; Ghosh, M.; Dutta, S. K. A potent tumoricidal co-drug 'Bet-CA'-an ester derivative of betulinic acid and dichloroacetate selectively and synergistically kills cancer cells. *Sci. Rep.*, **2015**, *5*, 7762–7771.
- (10) Devedjiev, Y.; Steussy, C. N.; Vassilyev, D. G. Crystal structure of an asymmetric complex of pyruvate dehydrogenase kinase 3 with lipoyl domain 2 and its biological implications. *J. Mol. Biol.*, **2007**, *370*, 407–416.
- (11) Koukourakis, M. I.; Giatromanolaki, A.; Bougioukas, G.; Sivridis, E. Lung cancer: a comparative study of metabolism related protein expression in cancer cells and tumor associated stroma. *Cancer Biol. Ther.*, **2007**, *6*, 1476–1479.
- (12) Wigfield, S. M.; Winter, S. C.; Giatromanolaki, A.; Taylor, J.; Koukourakis, M. L.; Harris, A. L. PDK-1 regulates lactate production in hypoxia and is associated with poor prognosis in head and neck squamous cancer. *Br. J. Cancer*, **2008**, *98*, 1975–1984.
- (13) Fujiwara, S.; Kawano, Y.; Yuki, H.; Okuno, Y.; Nosaka, K.; Mitsuya, H.; Hata, H. PDK1 inhibition is a novel therapeutic target in multiple myeloma. *Br. J. Cancer*, **2013**, *108*, 170–178.
- (14) Hur, H.; Xuan, Y.; Kim, Y. B.; Lee, G.; Shim, W.; Yun, J.; Ham, I. H.; Han, S. U. Expression of pyruvate dehydrogenase kinase-1 in gastric cancer as a potential therapeutic target. *Int. J. Oncol.*, **2013**, *42*, 44–54.
- (15) (a) Kim, J. W.; Tchernyshyov, I.; Semenza, G. L.; Dang, C. V. HIF-1-mediated expression of pyruvate dehydrogenase kinase: a metabolic switch required for cellular adaptation to hypoxia. *Cell Metab.*, **2006**, *3*, 177–185; (b) Papandreou, I.; Cairns, R. A.; Fontana, L.; Lim, A. L.; Denko, N. C. HIF-1 mediates adaptation to hypoxia by actively downregulating mitochondrial oxygen consumption. *Cell Metab.*, **2006**, *3*, 187–197; (c) Kim, J. W.; Gao, P.; Liu, Y. C.; Semenza, G. L.; Dang, C. V. Hypoxia-inducible factor 1 and dysregulated c-Myc cooperatively induce vascular endothelial growth factor and metabolic switches hexokinase 2 and pyruvate dehydrogenase kinase 1. *Mol. Cell. Biol.*, **2007**, *27*, 7381–7393.
- (16) Zhang, W.; Zhang, S. L.; Hu, X.; Tam, K. Y. Targeting tumor metabolism for cancer treatment: is pyruvate dehydrogenase kinases (PDKs) a viable anticancer target? *Int. J. Biol. Sci.*, **2015**, *11*, 1390–1400.
- (17) Aicher, T. D.; Anderson, R. C.; Beberitz, G. R.; Coppola, G. M.; Jewell, C. F.; Knorr, D. C.; Liu, C.; Sperbeck, D. M.; Brand, L. J.; Strohschein, R. J.; Gao, J.; Vinluan, C. C.; Shetty, S. S.; Dragland, C.; Kaplan, E. L.; DelGrande, D.; Islam, A.; Liu, X.; Lozito, R. J.; Maniara, W. M.; Walter, R. E.; Mann, W. R. (R)-3,3,3-Trifluoro-2-hydroxy-2-methylpropionamides are orally active inhibitors of pyruvate dehydrogenase kinase. *J. Med. Chem.*, **1999**, *42*, 2741–2746.
- (18) Morrell, J. A.; Orme, J.; Butlin, R. J.; Roche, T. E.; Mayers, R. M.; Kilgour, E. AZD7545 is a selective inhibitor of pyruvate dehydrogenase kinase 2. *Biochem. Soc. Trans.*, **2003**, *31*, 1168–1170.
- (19) Gahlot, P.; Kakkar, R. Docking modes of Pfz3 and its analogues into the lipamide binding site on PDHK2. *Int. Res. J. Pharm.*, **2011**, *1*, 33–41.
- (20) Moore, J. D.; Staniszewska, A.; Shaw, T.; Alessandro, J. D.; Davis, B.; Surgenor, A.; Baker, L.; Matassova, N.; Murray, J.; Macias, A.; Brough, P.; Wood, M.; Mahon, P. C. VER-246608, a novel pan-isoform ATP competitive inhibitor of pyruvate dehydrogenase kinase, disrupts Warburg metabolism and induces context-dependent cytostasis in cancer cells. *Oncotarget*, **2014**, *5*, 12862–12876.
- (21) Hiromasa, Y.; Roche, T. E. Pyruvate dehydrogenase kinase isoform 2 activity limited and further inhibited by slowing down the rate of dissociation of ADP. *Biochemistry*, **2008**, *47*, 2298–2311.
- (22) Kato, M.; Li, J.; Chuang, J. L.; Chuang, D. T. Distinct Structural Mechanisms for Inhibition of Pyruvate Dehydrogenase Kinase Isoforms by AZD7545, Dichloroacetate, and Radicol. *Structure*, **2007**, *15*, 992–1004.
- (23) Bonnet, S.; Archer, S. L.; Allalunis-Turner, J.; Haromy, A.; Beaulieu, C.; Thompson, R.; Lee, C. T.; Lopaschuk, G. D.; Puttagunta, L.; Bonnet, S.; Harry, G.; Hashimoto, K.; Porter, C. J.; Andrade, M. A.; Thebaud, B.; Michelakis, E. D. A mitochondria-K⁺ channel axis is suppressed in cancer and its normalization promotes apoptosis and inhibits cancer growth. *Cancer Cell*, **2007**, *11*, 37–51.
- (24) Aicher, T. D.; Anderson, R. C.; Gao, J.; Shetty, S. S.; Coppola, G. M.; Stanton, J. L.; Knorr, D. C.; Sperbeck, D. M.; Brand, L. J.; Vinluan, C. C.; Kaplan, E. L.; Dragland, C. J.; Tomaselli, H. C.; Islam, A.; Lozito, R. J.; Liu, X.; Maniara, W. M.; Fillers, W. S.; DelGrande, D.; Walter, R. E.; Mann, W. R. Secondary amides of (R)-3,3,3-trifluoro-2-hydroxy-2-methylpropionic acid as inhibitors of pyruvate dehydrogenase kinase. *J. Med. Chem.*, **2000**, *43*, 236–249.
- (25) Yang, Y. C.; Shang, P. H.; Cheng, C. M.; Wang, D. C.; Yang, P.; Zhang, F.; Li, T. W.; Lu, A. J.; Zhao, Y. F. Novel N-phenyl dichloroacetamide derivatives as anticancer reagents: design, synthesis and biological evaluation. *Eur. J. Med. Chem.*, **2010**, *45*, 4300–4306.
- (26) Li, T. W.; Yang, Y. C.; Cheng, C. M.; Tiwari, A. K.; Sodani, K.; Zhao, Y. F.; Abraham, I.; Chen, Z. S. Design, synthesis and biological evaluation of N-arylphenyl-2,2-dichloroacetamide analogues as anticancer agents. *Bioorg. Med. Chem. Lett.*, **2012**, *22*, 7268–7271.
- (27) Pathak, R. K.; Marrache, S.; Harn, D. A.; Dhar, S. Mito-DCA: a mitochondria targeted molecular scaffold for efficacious delivery of metabolic modulator dichloroacetate. *ACS Chem. Biol.*, **2014**, *9*, 1178–1187.

Table of content

